Flatness-based disturbance observer for exoskeleton robots under time-delayed contact forces

G. Rigatos[a] M. Abbaszadeh[b] J. Pomares[c]

[a]Unit of Industrial Automation
Industrial Systems Institute
26504, Rion Patras Greece
grigat@ieee.org

[b]Dept. ECS Engineering
Rensselaer Polytechnic Institute
12065, New York, USA
masouda@ualberta.ca

[c]Dept. of Systems Eng.
University of Alicante
03690, Alicante, Spain
jpomares@gcloud.ua.es

Abstract: The article proposes flatness-based control and a Kalman Filter-based disturbance observer for solving the control problem of a robotic exoskeleton under time-delayed exogenous disturbances. A two-link lower-limb robotic exoskeleton is used as a case study. It is proven that this robotic system is differentially flat. The robot is considered to be subject to unknown contact forces at its free-end which in turn generate unknown disturbance torques at its joints. It is shown that the dynamic model of the robotic exoskeleton can be transformed into the input-output linearized form and equivalently into the linear canonical Brunovsky form. This linearized description of the exoskeleton's dynamics is both controllable and observable. It allows for designing a stabilizing feedback controller with the use of the pole-placement (eigenvalues assignment) method. Moreover, it allows for solving the state estimation problem with the use of Kalman Filtering (the use of the Kalman Filter on the flatness-based linearized model of nonlinear dynamical systems is also known as Derivative-free nonlinear Kalman Filtering). Furthermore, (i) by extending the state vector of the exoskeleton after considering as additional state variables the additive disturbance torques which affect its joints and (ii) by redesigning the Kalman Filter as a disturbance observer, one can achieve the real-time estimation of the perturbations that affect this robotic system. Finally, by including in the controller of the exoskeleton additional terms that compensate for the estimated disturbance torques, the perturbations' effects can be eliminated and the precise tracking of reference trajectories by the joints of this robot can be ensured.

Keywords: lower-limb robotic exoskeleton, differential flatness properties, flatness-based control, Kalman Filtering, disturbance observer, time-delays compensation, global stability.

1 Introduction

The problem of reliable functioning of robotic systems under unmodelled time-delayed disturbance forces and torques is of significant difficulty and has been the subject of extensive research [1],2]. In the case of robotic exoskeletons, compensation of disturbances forces and torques is often pursued with disturbance observers. In [3] an overview is given about force and torque control techniques in rehabilitation robots. In [4] a 2-link lower-limb robotic exoskeleton is controlled with a sliding-mode controller, while an extended state observer is used to estimate disturbances. In [5] a 5-DOF upper limb robotic exoskeleton is considered and sliding mode control is applied jointly with an extended state observer which estimates disturbances. In [6] a 2-DOF lower-limb robotic exoskeleton is considered on which sliding-mode control and an extended state observer are applied, aiming at compensating for exogenous perturbations In [7] a 5-DOF upper limb robotic exoskeleton is considered and sliding mode control is used jointly with an extended state observer which estimates disturbances. In [8] adaptive fuzzy control jointly with a disturbance estimator are used in

a 5-DOF robotic exoskeleton. In [9] an adaptive control scheme jointly with a disturbance observer are used in the 7-DOF model of an upper-limb robotic exoskeleton to compensated for the effects of time-delayed perturbations. In [10] a backstepping controller is used jointly with a disturbance observer to eliminate the perturbations' impact in the model of a 2-DOF lower-limb robotic exoskeleton. In [11] a 4-DOF upper-link robotic exoskeleton is considered and a feedback controller designed in the s-frequency domain is used jointly with a disturbance estimator to ensure reliable functioning. In [12] a 2-DOF lower-limb robotic exoskeleton is analyzed and a PD feedback controller is applied to it jointly with an extended state observer which allows to estimate and compensate for lumped disturbances. In [13] an inverse dynamics controller is used jointly with a disturbance observer in the model of a 7-DOF upper-limb rehabilitation exoskeleton. In [14] a 3-DOF lower limb robotic exoskeleton is examined and an inverse dynamics controller is applied to it jointly with a dual Unscented Kalman Filter which performs both states and parameters estimation.

The use of disturbance observers in robotic exoskeletons is advantageous because it is computationally simple and ensures fast and precise estimation of unknown forces and torques. In [15] a 2-DOF lower-limb robotic exoskeleton is analyzed in which a fractional-order sliding-mode controller is applied together with a time-delays estimation scheme. In [16] a 2-DOF wrist rehabilitation exoskeleton is considered in which a PD feedback controller is applied jointly with an estimator of contact torques. In [17] a 3-DOF robotic exoskeleton is examined in which adaptive compliance control is used jointly with parameters' identification. In [18] an inverse dynamics controller is developed together with a disturbance observer which allows for joint torques' estimation in a 2-DOF lower-limb rehabilitation exoskeleton. In [19] a 5-DOF lower-limb robotic exoskeleton is considered in which a sliding-mode controller is applied together with a disturbance observer. In [20] a neural network is used as torques estimator in an upper-limb soft rehabilitation exoskeleton. In [21] an inverse dynamics controller is used in a 2-DOF upper-limb robotic exoskeleton jointly with a disturbance observer which allows for estimating and compensating for perturbation torques. In [22] a 6-DOF lower-limb robotic exoskeleton is controlled with the use of PD-type controllers while joint torques are computed through an optimization procedure related with energy variables of the robotic mechanism, Finally, in [23] a knee rehabilitation exoskeleton is considered in which sliding-mode control is applied together with a nonlinear disturbance observer.

In the present article, a flatness-based controller is developed jointly with a flatness-based disturbance observer for a 2-link lower-limb robotic exoskeleton which is subject to time-delayed torques. First, it is proven that the dynamic model of the 2-link robotic exoskeleton is differentially flat. This property means that all state variables and the control inputs of the robot can be written as differential functions of a subset of its state vector elements which are the flat outputs of the exoskeleton [24], [25], [26]. This property signifies also that the exoskeleton's dynamic model can be transformed into the input-output linearized form, or equivalently into the linear canonical (Brunovsky) form [27], [28]. The latter description of the dynamics of this robotic system is both controllable and observable. This allows for solving the stabilization and feedback control problem with the use of linear feedback control methods, such as the pole-placement (eigenvalues assignment) method. At the same time it allows for solving optimally the state estimation problem of the robot with Kalman Filtering [29], [30], [31]. The implementation of this filtering method on the flatness-based equivalent linearized model of the robotic exoskeleton and the use of flatness-based inverse transformations to obtain state estimates for the initial nonlinear state-space description of the robot is also known as Derivative-free nonlinear Kalman Filtering [32].

In the disturbance-free case, the use of the above-noted flatness-based controller jointly with the flatness-based implementation of Kalman Filtering would suffice to ensure stabilization of the exoskeleton and precise tracking of setpoints by its joints through feedback of the estimated state vector [1], [2]. However, the functioning of the exoskeleton comes against perturbations which are due to contact forces exerted at its free-end. The Jacobian matrix of the kinematic model of the exoskeleton shows how disturbance torques are in-turn developed at the joints of this robotic mechanism. These disturbance forces and torques may also be subject to time-delays. Both the mathematical description of these disturbance forces and torques

and the associated time-delays are unknown thus making their compensation by the exoskeleton's controller be a nontrivial problem. To treat this shortcoming, the article proposes the redesign of the aforementioned Kalman Filter as a disturbance observer that will allow for estimating in real-time the perturbation torques which affect the robot's joints [1], [2]. Using the estimates of these disturbance torques, additional terms can be included in the flatness-based controller of the exoskeleton thus finally achieving the complete elimination of the disturbances' impact and the precise tracking of setpoints by the exoskeleton's state variables.

The structure of the article is as follows: In Section 2 the dynamic model of the 2-link robotic exoskeleton being subject to unknown time-delayed contact forces and torques is analyzed. The differential flatness properties of this robotic system are proven. In Section 3 estimation of the disturbance torques which appear at the joints of the exoskeleton is performed with the use of a Kalman Filter-based disturbance observer. The estimated values of the perturbations are used in a differential flatness theory-based control scheme to stabilize the exoskeleton and to enable precise tracking of reference trajectories by its joints. In Section 4 the stability properties and the fine tracking performance of the proposed flatness-based control and disturbances' estimation scheme is further confirmed through simulation experiments. Finally, in Section 5, concluding remarks are stated. Moreover, an Appendix has been included in the end of the article to analyze the presented results on flatness-based control with the use of disturbance observers in the context of nonlinear control for dynamical systems with flat inputs.

2 Dynamic model of the robotic exoskeleton

2.1 State-space description of the robotic exoskeleton

A two-link lower-limb robotic exoskeleton is considered, as shown in Fig. 1. The dynamic model of the robotic exoskeleton can be also written in the concise form [33]

$$M(\theta)\ddot{\theta} + C(\theta,\dot{\theta})\dot{\theta} + G(\theta) = \tau \tag{1}$$

where the state-vector is $\theta = [\theta_1, \theta_2]^T$, the joints' torques vector is $\tau = [\tau_1, \tau_2]^T$, while the inertia matrix $M(\theta)$, the Coriolis matrix $C(\theta,\dot{\theta})$ and the gravitational forces matrix $G(\theta)$ are defined as follows [33]:

$$M(\theta) = \begin{pmatrix} m_1 d_1^2 + I_1 + m_2 l_1^2 + m_2 d_1^2 + 2 m_2 l_1 d_2 cos(\theta_2) + I_2 & -m_2 d_2^2 - m_2 l_1 d_2 cos(\theta_2) - I_2 \\ -m_2 d_2^2 - m_2 l_1 d_2 cos(\theta_2) - I_2 & m_2 d_2^2 + I_2 \end{pmatrix} \tag{2}$$

$$C(\theta,\dot{\theta})\dot{\theta} = \begin{pmatrix} -m_2 l_1 d_2 sin(\theta_2)\dot{\theta}_2(2\dot{\theta}_1 - \dot{\theta}_2) \\ m_2 l_1 d_2 sin(\theta_2)\dot{\theta}_1^2 \end{pmatrix} \quad G(\theta) = \begin{pmatrix} (m_1 g d_1 + m_2 g l_1) sin(\theta_1) + m_2 g d_2 sin(\theta_1 - \theta_2) \\ m_2 g d_2 sin(\theta_1 - \theta_2) \end{pmatrix} \tag{3}$$

Using that the symmetric inertia matrix $M(\theta)$ is

$$M = \begin{pmatrix} M_{11} & M_{12} \\ M_{21} & M_{22} \end{pmatrix} \tag{4}$$

and that the determinant of $M(\theta)$ is $detM = M_{11}M_{22} - M_{12}^2$, the inverse of $M(\theta)$ is

$$M^{-1} = \begin{pmatrix} \frac{M_{22}}{M_{11}M_{22} - M_{12}^2} & \frac{-M_{12}}{M_{11}M_{22} - M_{12}^2} \\ \frac{-M_{21}}{M_{11}M_{22} - M_{12}^2} & \frac{M_{11}}{M_{11}M_{22} - M_{12}^2} \end{pmatrix} \tag{5}$$

Thus the dynamic model of the exoskeleton robot is written as

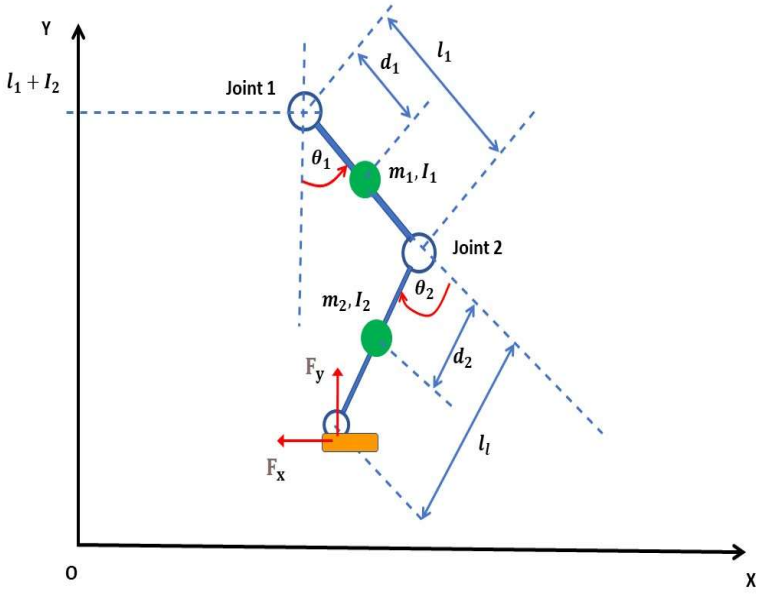

Figure 1: Diagram of the two-link lower-limb robotic exoskeleton with forces exerted at its free end

$$\ddot{\theta} = -M^{-1}(\theta)[C(\theta,\dot{\theta})\dot{\theta} + G(\theta)] + M^{-1}(\theta)\tau \tag{6}$$

By performing operations between the individual matrices one arrives at the state-space description

$$\begin{pmatrix} \ddot{\theta}_1 \\ \\ \ddot{\theta}_2 \end{pmatrix} = \begin{pmatrix} \frac{-M_{22}(C_1+G_1)+M_{12}(C_2+G_2)}{M_{11}M_{22}-M_{12}^2} \\ \\ \frac{M_{12}(C_1+G_1)-M_{11}(C_2+G_2)}{M_{11}M_{22}-M_{12}^2} \end{pmatrix} + \begin{pmatrix} \frac{M_{22}}{M_{11}M_{22}-M_{12}^2} & \frac{-M_{12}}{M_{11}M_{22}-M_{12}^2} \\ \\ \frac{-M_{21}}{M_{11}M_{22}-M_{12}^2} & \frac{M_{11}}{M_{11}M_{22}-M_{12}^2} \end{pmatrix} \begin{pmatrix} \tau_1 \\ \\ \tau_2 \end{pmatrix} \tag{7}$$

The state variables of the exoskeleton are $x_1 = \theta_1$, $x_2 = \dot{\theta}_1]$, $x_3 = \theta_2$ and $x_4 = \dot{\theta}_2$. In case that no contact forces are exerted on the free-end of the robotic exoskeleton the associated state-space model is given by

$$\dot{x}_1 = x_2 \tag{8}$$

$$\dot{x}_2 = \frac{-M_{22}(C_1+G_1)+M_{12}(C_2+G_2)}{M_{11}M_{22}-M_{12}^2} + \frac{M_{22}}{M_{11}M_{22}-M_{12}^2}\tau_1 + \frac{M_{12}}{M_{11}M_{22}-M_{12}^2}\tau_2 \tag{9}$$

$$\dot{x}_3 = x_4 \tag{10}$$

$$\dot{x}_4 = \frac{M_{12}(C_1+G_1)-M_{11}(C_2+G_2)}{M_{11}M_{22}-M_{12}^2} - \frac{M_{21}}{M_{11}M_{22}-M_{12}^2}\tau_1 + \frac{M_{11}}{M_{11}M_{22}-M_{12}^2}\tau_2 \tag{11}$$

With reference to the diagram of Fig. 1 the coordinates of the free-end of the two-link robotic exoskeleton are

$$\begin{aligned} x &= x_0 + l_1 sin(\theta_1) + l_2 sin(\theta_1 - \theta_2) \\ y &= l_1 + l_2 - l_1 cos(\theta_1) - l_2 cos(\theta_1 - \theta_2) \end{aligned} \tag{12}$$

The associated Jacobian matrix, having as elements the partial derivatives of x and y with respect to the joint angles of the robotic exoskeleton θ_1 and θ_2 are:

$$J = \begin{pmatrix} l_1 cos(\theta_1) + l_2 cos(\theta_1 - \theta_2) & -l_2 cos(\theta_1 - \theta_2) \\ l_1 sin(\theta_1) - l_2 sin(\theta_1 - \theta_2) & -l_2 sin(\theta_1 - \theta_2) \end{pmatrix} \tag{13}$$

It is considered that the following forces are exerted on the free-end of the exoskeleton

$$\begin{array}{c} F_x = k_{11}\theta_1(t - \tau_{11}) + k_{21}\theta_2(t - \tau_{21}) \\ F_y = k_{12}\theta_1(t - \tau_{21}) + k_{22}\theta_2(t - \tau_{22}) \end{array} \tag{14}$$

that is the forces are expressed as the sum of the products of the time-delayed turn angles of the joints with elasticity coefficients. The torques which are transferred to the joints of the exoskeleton are given by $T = J^T F$ where $F = [F_x, F_y]^T$. Both the elasticity coefficients k_{11}, k_{21}, k_{12}, k_{22} and the time-delay coefficients τ_{11}, τ_{21}, τ_{12}, τ_{22} are taken to be unknown.

The torques which are transferred to the joints of the robotic exoskeleton are given by

$$J^T F = \begin{pmatrix} l_1 cos(\theta_1) + l_2 cos(\theta_1 - \theta_2) & -l_2 cos(\theta_1 - \theta_2) \\ l_1 sin(\theta_1) - l_2 sin(\theta_1 - \theta_2) & -l_2 sin(\theta_1 - \theta_2) \end{pmatrix}^T \begin{pmatrix} k_{11}\theta_1(t - \tau_{11}) + k_{21}\theta_2(t - \tau_{21}) \\ k_{12}\theta_1(t - \tau_{21}) + k_{22}\theta_2(t - \tau_{22}) \end{pmatrix} \tag{15}$$

By approximating the time-delayed terms of the contact forces through Taylor series expansion, that is

$$\begin{array}{c} F_x = k_{11}\theta_1(t) - k_{11}\tau_{11}\dot{\theta_1}(t) + k_{21}\theta_2(t) - k_{21}\tau_{21}\dot{\theta_2}(t) \\ F_y = k_{12}\theta_1(t) - k_{12}\tau_{12}\dot{\theta_2}(t) + k_{22}\theta_2(t) - k_{22}\tau_{22}\dot{\theta_2}(t) \end{array} \tag{16}$$

the torques which are transferred to the joint of the robotic exoskeleton are given by

$$J^T F = \begin{pmatrix} l_1 cos(\theta_1) + l_2 cos(\theta_1 - \theta_2) & -l_2 cos(\theta_1 - \theta_2) \\ l_1 sin(\theta_1) - l_2 sin(\theta_1 - \theta_2) & -l_2 sin(\theta_1 - \theta_2) \end{pmatrix}^T \begin{pmatrix} k_{11}\theta_1(t) - k_{11}\tau_{11}\dot{\theta_1}(t) + k_{21}\theta_2(t) - k_{21}\tau_{21}\dot{\theta_2}(t) \\ k_{12}\theta_1(t) - k_{12}\tau_{12}\dot{\theta_2}(t) + k_{22}\theta_2(t) - k_{22}\tau_{22}\dot{\theta_2}(t) \end{pmatrix} \tag{17}$$

or equivalently using the state variables notation $x_1 = \theta_1$, $x_2 = \dot{\theta}_1$, $x_3 = \theta_3$, $x_4 = \dot{\theta}_4$ one obtains

$$J^T F = \begin{pmatrix} l_1 cos(x_1) + l_2 cos(x_1 - x_3) & l_1 sin(x_1) - l_2 sin(x_1 - x_3) \\ -l_2 cos(x_1 - x_3) & -l_2 sin(x_1 - x_3) \end{pmatrix} \begin{pmatrix} k_{11}x_1 - k_{11}\tau_{11}x_2 + k_{21}x_3 - k_{21}\tau_{21}x_4 \\ k_{12}x_1 - k_{12}\tau_{12}x_2 + k_{22}x_3 - k_{22}\tau_{22}x_4 \end{pmatrix} \tag{18}$$

By denoting the torques which are transferred to the joints of the robotic exoskeleton as

$$\begin{array}{c} \tilde{\tau}_1 = [l_1 cos(x_1) + l_2 cos(x_1 - x_3)[k_{11}x_1 - k_{11}\tau_{11}x_2 + k_{21}x_3 - k_{21}\tau_{21}x_4] + \\ + [l_1 sin(x_1) - l_2 sin(x_1 - x_3)][k_{12}x_1 - k_{12}\tau_{12}x_2 + k_{22}x_3 - k_{22}\tau_{22}x_4] \end{array} \tag{19}$$

$$\begin{array}{c} \tilde{\tau}_2 = [-l_2 cos(x_1 - x_3)][k_{11}x_1 - k_{11}\tau_{11}x_2 + k_{21}x_3 - k_{21}\tau_{21}x_4] + \\ + [-l_2 sin(x_1 - x_3)][k_{12}x_1 - k_{12}\tau_{12}x_2 + k_{22}x_3 - k_{22}\tau_{22}x_4] \end{array} \tag{20}$$

the state-space model of the robotic exoskeleton is rewritten as

$$\dot{x}_1 = x_2 \tag{21}$$

$$\dot{x}_2 = \frac{-M_{22}(C_1+G_1)+M_{12}(C_2+G_2)}{M_{11}M_{22}-M_{12}^2} + \frac{M_{22}}{M_{11}M_{22}-M_{12}^2}(\tau_1 + \tilde{\tau}_1) - \frac{M_{12}}{M_{11}M_{22}-M_{12}^2}(\tau_2 + \tilde{\tau}_2) \tag{22}$$

$$\dot{x}_3 = x_4 \tag{23}$$

$$\dot{x}_4 = \frac{M_{12}(C_1+G_1)-M_{11}(C_2+G_2)}{M_{11}M_{22}-M_{12}^2} - \frac{M_{21}}{M_{11}M_{22}-M_{12}^2}(\tau_1 + \tilde{\tau}_1) - \frac{M_{11}}{M_{11}M_{22}-M_{12}^2}(\tau_2 + \tilde{\tau}_2) \tag{24}$$

Thus, the model of the robotic exoskeleton under the effects of time-delayed external forces and torques is written in the concise form

$$\dot{x} = f(x) + g(x)u \tag{25}$$

where $x \in R^{4\times 1}$, $f(x) \in R^{4\times 1}$, $g(x) \in R^{4\times 2}$ and $u \in R^{2\times 1}$, with the drift vector $f(x)$ to be given by

$$f(x) = \begin{pmatrix} x_2 \\ \frac{-M_{22}(C_1+G_1)+M_{12}(C_2+G_2)}{M_{11}M_{22}-M_{12}^2} + \frac{M_{22}}{M_{11}M_{22}-M_{12}^2}\tilde{\tau}_1 + \frac{M_{12}}{M_{11}M_{22}-M_{12}^2}\tilde{\tau}_2 \\ x_4 \\ \frac{M_{12}(C_1+G_1)-M_{11}(C_2+G_2)}{M_{11}M_{22}-M_{12}^2} - \frac{M_{21}}{M_{11}M_{22}-M_{12}^2}\tilde{\tau}_1 + \frac{M_{11}}{M_{11}M_{22}-M_{12}^2}\tilde{\tau}_2 \end{pmatrix} \tag{26}$$

while the control inputs gain matrix $g(x)$ is given by

$$g(x) = \begin{pmatrix} 0 & 0 \\ \frac{M_{22}}{M_{11}M_{22}-M_{12}^2} & \frac{M_{12}}{M_{11}M_{22}-M_{12}^2} \\ 0 & 0 \\ -\frac{M_{21}}{M_{11}M_{22}-M_{12}^2} & \frac{M_{11}}{M_{11}M_{22}-M_{12}^2} \end{pmatrix} \tag{27}$$

Equivalent the state-space model of the robotic exoskeleton under time-delayed external forces is given by

$$\begin{aligned} \ddot{x}_1 &= f_2(x) + g_{21}(x)u_1 + g_{22}(x)u_2 \\ \ddot{x}_3 &= f_4(x) + g_{41}(x)u_1 + g_{42}(x)u_2 \end{aligned} \tag{28}$$

2.2 Stabilizing feedback control for the robotic exoskeleton

In Eq. (30) the following transformed control inputs are defined

$$\begin{aligned} v_1 &= f_2(x) + g_{21}(x)u_1 + g_{22}(x)u_2 \\ v_2 &= f_4(x) + g_{41}(x)u_1 + g_{42}(x)u_2 \end{aligned} \tag{29}$$

Then, the dynamic model of the exoskeleton is written as

$$\ddot{x}_1 = v_1 \quad \ddot{x}_3 = v_2 \tag{30}$$

The dynamic model of the exoskeleton robot can be also written in the canonical (Brunovsky) form

$$\begin{pmatrix} \dot{x}_1 \\ \dot{x}_2 \\ \dot{x}_3 \\ \dot{x}_4 \end{pmatrix} = \begin{pmatrix} 0 & 1 & 0 & 0 \\ 0 & 0 & 0 & 0 \\ 0 & 0 & 0 & 1 \\ 0 & 0 & 0 & 0 \end{pmatrix} \begin{pmatrix} x_1 \\ x_2 \\ x_3 \\ x_4 \end{pmatrix} + \begin{pmatrix} 0 & 0 \\ 1 & 0 \\ 0 & 0 \\ 0 & 1 \end{pmatrix} \begin{pmatrix} v_1 \\ v_2 \end{pmatrix} \tag{31}$$

and the associated measurement equation is

$$\begin{pmatrix} x_1^m \\ x_3^m \end{pmatrix} = \begin{pmatrix} 1 & 0 & 0 & 0 \\ 0 & 0 & 1 & 0 \end{pmatrix} \begin{pmatrix} x_1 \\ x_2 \\ x_3 \\ x_4 \end{pmatrix} \tag{32}$$

The stabilizing feedback control is computed as follows

$$\begin{aligned} v_1 &= \ddot{x}_1^d - \tilde{k}_{11}(\dot{x}_1 - \dot{x}_1^d) + \tilde{k}_{12}(x_1 - x_1^d) \\ v_2 &= \ddot{x}_3^d - \tilde{k}_{13}(\dot{x}_3 - \dot{x}_3^d) + \tilde{k}_{23}(x_3 - x_3^d) \end{aligned} \tag{33}$$

and by denoting the tracking error variables as $e_1 = x_1 - x_1^d$ and $e_3 = x_3 - x_3^d$ one has the tracking error dynamics

$$\begin{matrix} \ddot{e}_1 + \tilde{k}_{11}\dot{e}_1 + \tilde{k}_{12}e_1 = 0 \\ \ddot{e}_3 + \tilde{k}_{13}\dot{e}_3 + \tilde{k}_{23}e_3 = 0 \end{matrix} \tag{34}$$

Through suitable selection of the feedback gains $\tilde{k}_{11}$, $\tilde{k}_{21}$, $\tilde{k}_{13}$ and $\tilde{k}_{23}$, it can be assured that the associated characteristic polynomials are Hurwitz stable

$$\begin{matrix} p_1(s) = s^2 + \tilde{k}_{11}s + \tilde{k}_{12} = 0 \\ p_2(s) = s^2 + \tilde{k}_{13}s + \tilde{k}_{23} = 0 \end{matrix} \tag{35}$$

This ensures that the tracking error variables will converge asymptotically to 0, that is

$$\begin{matrix} lim_{t\to\infty}e_1(t) = 0 & lim_{t\to\infty}e_3(t) = 0 \\ lim_{t\to\infty}x_1(t) = x_1^d(t) & lim_{t\to\infty}x_3(t) = x_3^d(t) \end{matrix} \tag{36}$$

The control inputs which are applied to the initial nonlinear model of the robotic exoskeleton are given by

$$\begin{pmatrix} v_1 \\ v_2 \end{pmatrix} = \begin{pmatrix} g_{11}(x) & g_{12}(x) \\ g_{21}(x) & g_{22}(x) \end{pmatrix}^{-1} \begin{pmatrix} v_1 - f_1(x) \\ v_2 - f_2(x) \end{pmatrix} \tag{37}$$

2.3 Differential flatness properties of the model of the robotic exoskeleton

It will be proven that the dynamic model of the robotic exoskeleton under time-delayed external forces is a differentially flat system with flat outputs $y_1 = x_1$ and $y_2 = x_3$ [1], [2]. The dynamic model of the robotic exoskeleton has been given in the form

$$\begin{matrix} \ddot{x}_1 = f_2(x) + g_{21}(x)u_1 + g_{22}(x)u_2 \\ \ddot{x}_3 = f_4(x) + g_{41}(x)u_1 + g_{42}(x)u_2 \end{matrix} \tag{38}$$

The state vector of the robotic exoskeleton is re-defined as $z = [z_1, z_2, z_3, z_4]^T = [x_1, \dot{x}_1, x_3, \dot{x}_3]^T$, thus the associated dynamic model can be written as

$$\begin{matrix} \dot{z}_1 = z_2 \\ \dot{z}_2 = f_2(z) + g_{21}(z)u_1 + g_{22}(z)u_2 \\ \dot{z}_3 = z_4 \\ \dot{z}_4 = f_4(z) + g_{41}(z)u_1 + g_{42}(z)u_2 \end{matrix} \tag{39}$$

It will be demonstrated that the robotic exoskeleton is a differentially flat system with flat outputs $y_1 = z_1$ and $y_2 = z_3$. This signifies that all state variables of the robot and its control inputs can be written as differential functions of the system's flat outputs, (ii) the state variables and their derivatives are differentially independent, which means that they are not connected between them through a relation in the form of an homogeneous ordinary differential equation [1].

From the first and third row of the state-space model one has

$$z_2 = \dot{z}_1 \quad z_4 = \dot{z_3} \tag{40}$$

which signifies that state variables z_2 and z_4 are differential functions of the system's flat outputs. Moreover, from the second and fourth rows of the state-space model one has a system of two equation with respect to u_1 and u_2 which gives

$$\begin{pmatrix} u_1 \\ u_2 \end{pmatrix} = \begin{pmatrix} g_{21}(z) & g_{22}(z) \\ g_{41}(z) & g_{42}(z) \end{pmatrix}^{-1} \begin{pmatrix} \ddot{z}_1 - f_1(z) \\ \ddot{z}_3 - f_3(z) \end{pmatrix} \tag{41}$$

which signifies that the control inputs u_1 and u_2 are also differential functions of the system's flat outputs. Consequently, the robotic exoskeleton is a differentially flat system. By defining setpoints z_1^d and z_3^d it is straightforward to compute setpoints z_2^d and z_4^d as well.

3 Estimation of perturbations with the use of a disturbance observer

In the dynamic model of the exoskeleton robot, the disturbance terms which are due to the time-delayed external forces are described as

$$\tilde{d}_1 = \frac{M_{22}}{M_{11}M_{22}-M_{12}^2}\tilde{\tau}_1 - \frac{M_{12}}{M_{11}M_{22}-M_{12}^2}\tilde{\tau}_2 \tag{42}$$

$$\tilde{d}_2 = -\frac{M_{21}}{M_{11}M_{22}-M_{12}^2}\tilde{\tau}_1 + \frac{M_{11}}{M_{11}M_{22}-M_{12}^2}\tilde{\tau}_2 \tag{43}$$

The new drift vector $\tilde{f}(x)$ in the model of the exoskeleton is defined as

$$\tilde{f}(x) = \begin{pmatrix} x_2 \\ \frac{-M_{22}(C_1+G_1)+M_{12}(C_2+G_2)}{M_{11}M_{22}-M_{12}^2} \\ x_4 \\ \frac{M_{12}(C_1+G_1)-M_{11}(C_2+G_2)}{M_{11}M_{22}-M_{12}^2} \end{pmatrix} \tag{44}$$

Thus, the dynamic model of the exoskeleton is written as

$$\begin{aligned} \ddot{x}_1 &= \tilde{f}_2(x) + g_{21}(x)u_1 + g_{22}(x)u_2 + \tilde{d}_1 \\ \ddot{x}_3 &= \tilde{f}_4(x) + g_{41}(x)u_1 + g_{42}(x)u_2 + \tilde{d}_2 \end{aligned} \tag{45}$$

Next, by considering that the dynamics of the disturbance terms is given by the second order time-derivative of $\tilde{d}_1$, and $\tilde{d}_2$, one has

$$\dddot{\tilde{d}}_1 = f_{\tilde{d}_1} \quad \dddot{\tilde{d}}_2 = f_{\tilde{d}_2} \tag{46}$$

This assumption is reasonable because every function can be described by its n-th order derivative and the associated initial conditions. If estimation is to be carried out with the use of a convergent filtering method then knowledge of initial conitiosn becomes obsolete. By considering the disturbance terms $\tilde{d}_1$ and $\tilde{d}_2$ and their time-derivatives as additional state variables one arrives at an extended state-space description of the robotic exoskeleton. Actually, the following state variables are defined in an extended state-space description of this robotic system: $z_1 = x_1$, $z_2 = \dot{x}_1$, $z_3 = x_3$, $z_4 = \dot{x}_3$, $z_5 = \tilde{d}_1$, $z_6 = \dot{\tilde{d}}_1$, $z_7 = \tilde{d}_2$ and $z_8 = \dot{\tilde{d}}_2$. Thus,the extended state-space model of the robotic exoskeleton is written as:

$$\begin{pmatrix} \dot{z}_1 \\ \dot{z}_2 \\ \dot{z}_3 \\ \dot{z}_4 \\ \dot{z}_5 \\ \dot{z}_6 \\ \dot{z}_7 \\ \dot{z}_8 \end{pmatrix} = \begin{pmatrix} 0 & 1 & 0 & 0 & 0 & 0 & 0 & 0 \\ 0 & 0 & 0 & 0 & 1 & 0 & 0 & 0 \\ 0 & 0 & 0 & 1 & 0 & 0 & 0 & 0 \\ 0 & 0 & 0 & 0 & 0 & 0 & 1 & 0 \\ 0 & 0 & 0 & 0 & 0 & 1 & 0 & 0 \\ 0 & 0 & 0 & 0 & 0 & 0 & 0 & 0 \\ 0 & 0 & 0 & 0 & 0 & 0 & 0 & 1 \\ 0 & 0 & 0 & 0 & 0 & 0 & 0 & 0 \end{pmatrix} \begin{pmatrix} z_1 \\ z_2 \\ z_3 \\ z_4 \\ z_5 \\ z_6 \\ z_7 \\ z_8 \end{pmatrix} + \begin{pmatrix} 0 & 0 & 0 & 0 \\ 1 & 0 & 0 & 0 \\ 0 & 0 & 0 & 0 \\ 0 & 1 & 0 & 0 \\ 0 & 0 & 0 & 0 \\ 0 & 0 & 1 & 0 \\ 0 & 0 & 0 & 0 \\ 0 & 0 & 0 & 1 \end{pmatrix} \begin{pmatrix} v_1 \\ v_2 \\ f_{\tilde{d}_1} \\ f_{\tilde{d}_2} \end{pmatrix} \tag{47}$$

and the associated measurement equation becomes

$$\begin{pmatrix} z_1^m \\ z_3^m \end{pmatrix} = \begin{pmatrix} 1 & 0 & 0 & 0 & 0 & 0 & 0 & 0 \\ 0 & 0 & 1 & 0 & 0 & 0 & 0 & 0 \end{pmatrix} \begin{pmatrix} z_1 \\ z_2 \\ z_3 \\ z_4 \\ z_5 \\ z_6 \\ z_7 \\ z_8 \end{pmatrix} \tag{48}$$

The extended state-space model of the robotic exoskeleton is concisely written as:

$$\begin{array}{c} \dot{z} = A_e z + B_e v + w \\ z^m = C_e Z + v \end{array} \tag{49}$$

where w is the vector of process noise and v is the vector of measurement noise. Next, the non-measurable state variables of the robotic exoskeleton, as well as the disturbance terms $\tilde{d}_1$ and $\tilde{d}_2$ can be estimated with the use of a disturbance observer, which is written first in the following continuous-time form

$$\begin{array}{c} \dot{\hat{z}} = A_{e,o}\hat{z} + B_{e,o}v_e + K_f(z^m - \hat{z}^m) \\ \hat{z}^m = C_{e,o}\hat{z} \end{array} \tag{50}$$

where matrices $A_{e,o}$, $B_{e,o}$ and $C_{e,o}$ are defined as follows:

$$A_{e,o} = \begin{pmatrix} 0 & 1 & 0 & 0 & 0 & 0 & 0 & 0 \\ 0 & 0 & 0 & 0 & 1 & 0 & 0 & 0 \\ 0 & 0 & 0 & 1 & 0 & 0 & 0 & 0 \\ 0 & 0 & 0 & 0 & 0 & 0 & 1 & 0 \\ 0 & 0 & 0 & 0 & 0 & 1 & 0 & 0 \\ 0 & 0 & 0 & 0 & 0 & 0 & 0 & 0 \\ 0 & 0 & 0 & 0 & 0 & 0 & 0 & 1 \\ 0 & 0 & 0 & 0 & 0 & 0 & 0 & 0 \end{pmatrix} \quad B_{e,o} = \begin{pmatrix} 0 & 0 \\ 1 & 0 \\ 0 & 0 \\ 0 & 1 \\ 0 & 0 \\ 0 & 0 \\ 0 & 0 \\ 0 & 0 \end{pmatrix} \quad C_{e,o}^T = \begin{pmatrix} 1 & 0 \\ 0 & 0 \\ 0 & 1 \\ 0 & 0 \\ 0 & 0 \\ 0 & 0 \\ 0 & 0 \\ 0 & 0 \end{pmatrix} \tag{51}$$

The observer's gain K_f is computed through Kalman Filter's recursion after expressing Eq. (50) in discrete-time form. To this end, matrices $A_{e,o}$, $B_{e,o}$ and $C_{e,}$ are substituted by their discrete-time equivalents A_d, B_d, C_d after using common discretization methods. The Kalman Filter's recursion consists of a measurement-update stage and of a time-update stage:

measurement update:

$$\begin{array}{c} K_f(k) = P^-(k)C_d^T[C_d P^-(k) C_d^T + R]^{-1} \\ \hat{z}(k) = \hat{z}^-(k) + K_f(k)[z_m - \hat{z}_m] \\ P(k) = P^-(k) - K_f(k) C_d P^-(k) \end{array} \tag{52}$$

time update:

$$\begin{array}{c} P^-(k+1) = A_d P(k) A_d^T + Q \\ \hat{z}^-(k+1) = A_d \hat{z}(k) + B_d v(k) \end{array} \tag{53}$$

In the equations of the Kalman Filter's recursion P is the a-posteriori state vector's error covariance matrix (after receiving the output measurements at the k-th sampling interval), and P^- is the a-priori state vector's error covariance matrix (before receiving the output measurements at the k-th sampling interval). Besides Q denotes the process noise covariance matrix, while R is the measurement noise covariance matrix. Once the estimates $\hat{\tilde{d}}_1$ and $\hat{\tilde{d}}_2$ of the disturbance terms $\tilde{d}_1$ and $\tilde{d}_2$ are obtained the stabilizing feedback control becomes

$$\begin{array}{l} v_1 = \ddot{x}_1^d - \tilde{k}_{11}(\dot{x}_1 - \dot{x}_1^d) - \tilde{k}_{21}(x_1 - \tilde{x}_1^d) - \hat{\tilde{d}}_1 \\ v_2 = \ddot{x}_3^d - \tilde{k}_{12}(\dot{x}_3 - \dot{x}_3^d) - \tilde{k}_{23}(x_3 - \tilde{x}_3^d) - \hat{\tilde{d}}_3 \end{array} \tag{54}$$

The selection of the feedback gains that appear in Eq. (54) has already been explained in the end of subsection 2.2. The control inputs which are applied to the initial nonlinear model of the robotic exoskeleton are given by

$$\begin{pmatrix} v_1 \\ v_2 \end{pmatrix} = \begin{pmatrix} g_{11}(x) & g_{12}(x) \\ g_{21}(x) & g_{22}(x) \end{pmatrix}^{-1} \begin{pmatrix} v_1 - \tilde{f}_1(x) \\ v_2 - \tilde{f}_2(x) \end{pmatrix} \tag{55}$$

4 Simulation tests

The performance of the proposed flatness-bases control scheme, has been tested in the dynamic model of the previously analyzed lower-limb 2-link robotic exoskeleton. The use of a Kalman Filter-based disturbance observer has allowed to estimate time-delayed disturbance torques that were applied on the robot's joints. Using these estimates, additional control terms have been included in the controller of the robotic exoskeleton, thus allowing finally to compensate for the perturbations' effects. The measured state vector elements where the two turn angles of the joints that is $x_1 = \theta_1$ and $x_3 = \theta_2$. The obtained results are depicted in Fig. 2 to Fig. 9.

The advantages of using a global linearization-based control method for the dynamic model of the robotic exoskeleton are outlined as follows: (i) the transformation that is performed on the robotic system's state-space model is an exact one and does not introduce any modelling errors (ii) by expressing the dynamic model of the robotic exoskeleton into the linear canonical form it is assured that the separation principle holds and that the design of the control problem can be solved independently from the design of the state-observer, (iii) by using the Kalman Filter as a disturbance observer the estimation and compensation of perturbation terms that affect the exoskleton's model is achieved and thus the robustness of the control scheme is improved (iv) The robustness properties of the control method are equivalent to those of LQG (Linear Quadratic Gaussian) control, (v) by using the Kalman Filter as a disturbance observer, optimality in the estimation of the perturbation torques is assured.

To elaborate on the tracking performance and on the robustness of the proposed flatness-based control method for the robotic exoskeleton the following Tables I to IV are given, which provide information about the accuracy of tracking of the reference setpoints by the state variables x_1, x_3 of the robot, as well as about the accuracy of estimation of the cumulative disturbance inputs $\tilde{d}_1$, $\tilde{d}_2$: (i) Table I, under time-delay coefficients denoted by the set $\tau_d = [\tau_{d_1}1, \tau_{d_2}, \tau_{d_3}1, \tau_{d_4}2] = [0.5, 0.7, 0.6, 0.4]$ sec, (ii) Table II, under time-delay coefficients denoted by the set $2{\cdot}\tau_d$, (iii) Table III, under time-delay coefficients denoted by the set $3{\cdot}\tau_d$, (iv) Table IV, under time-delay coefficients denoted by the set $4{\cdot}\tau_d$.

Table I

Tracking RMSE for the robot under time-delay set τ_d

	$RMSE_{x_1}$	$RMSE_{x_3}$	$RMSE_{\tilde{d}_1}$	$RMSE_{\tilde{d}_2}$
test_1	0.0038	0.0014	0.0307	0.0391
test_2	0.0041	0.0066	0.0214	0.0626
test_3	0.0084	0.0015	0.0779	0.0449
test_4	0.0040	0.0043	0.0709	0.0506
test_5	0.0031	0.0018	0.0234	0.0564
test_6	0.0036	0.0039	0.0253	0.0218
test_7	0.0015	0.0029	0.0002	0.0004
test_8	0.0018	0.0038	0.0001	0.0002

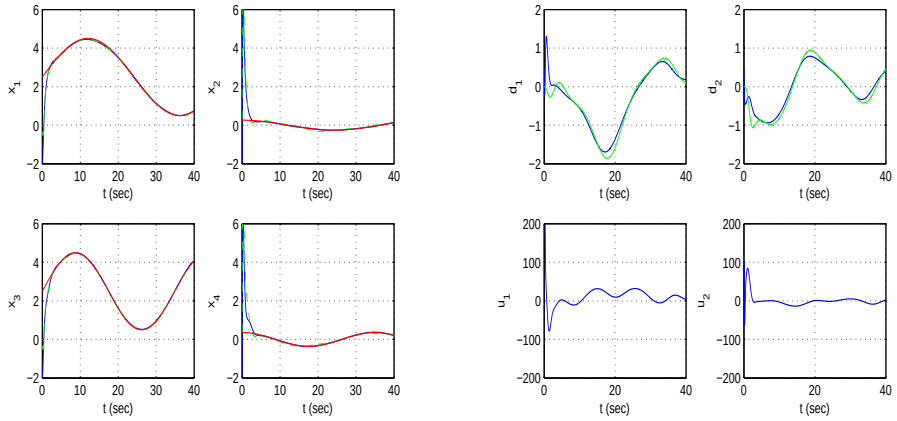

(a) **(b)**

Figure 2: Tracking of setpoint 1 by the 2-link robotic exoskeleton (a) Convergence of the state variables x_1 to x_4 (blue lines) to the reference setpoints (red lines) and KF-estimated state variables (green lines), (b) top diagrams: Kalman Filter-based estimation of disturbance torques $\tilde{d}_1$ and $\tilde{d}_2$ (green lines) and real values of these perturbations (blue lines), bottom diagrams: control inputs (torques) u_1 and u_2 applied to the joints of the exoskeleton

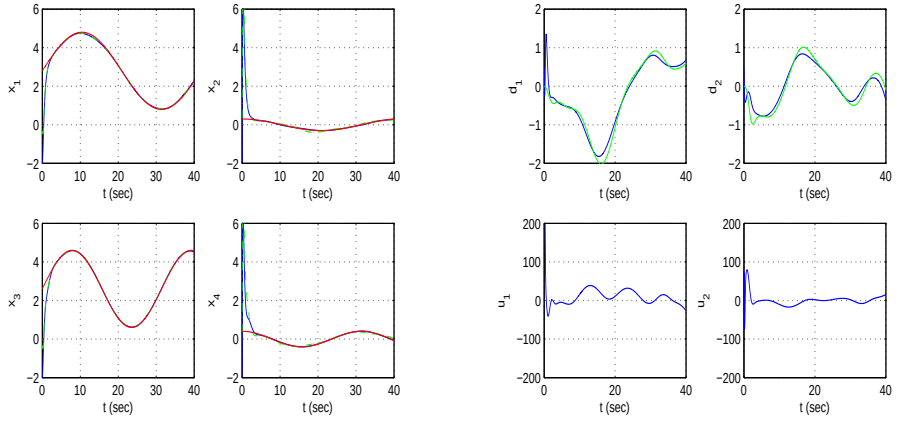

(a) **(b)**

Figure 3: Tracking of setpoint 2 by the 2-link robotic exoskeleton (a) Convergence of the state variables x_1 to x_4 (blue lines) to the reference setpoints (red lines) and KF-estimated state variables (green lines), (b) top diagrams: Kalman Filter-based estimation of disturbance torques $\tilde{d}_1$ and $\tilde{d}_2$ (green lines) and real values of these perturbations (blue lines), bottom diagrams: control inputs (torques) u_1 and u_2 applied to the joints of the exoskeleton

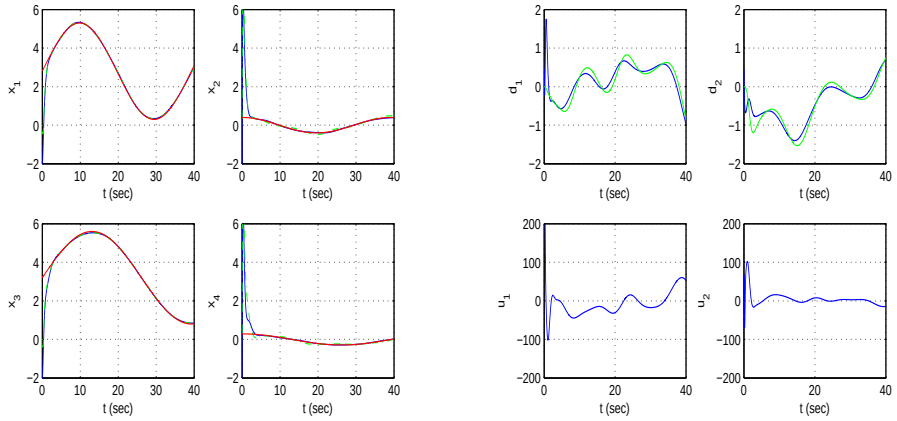

(a) **(b)**

Figure 4: Tracking of setpoint 3 by the 2-link robotic exoskeleton (a) Convergence of the state variables x_1 to x_4 (blue lines) to the reference setpoints (red lines) and KF-estimated state variables (green lines), (b) top diagrams: Kalman Filter-based estimation of disturbance torques $\tilde{d}_1$ and $\tilde{d}_2$ (green lines) and real values of these perturbations (blue lines), bottom diagrams: control inputs (torques) u_1 and u_2 applied to the joints of the exoskeleton

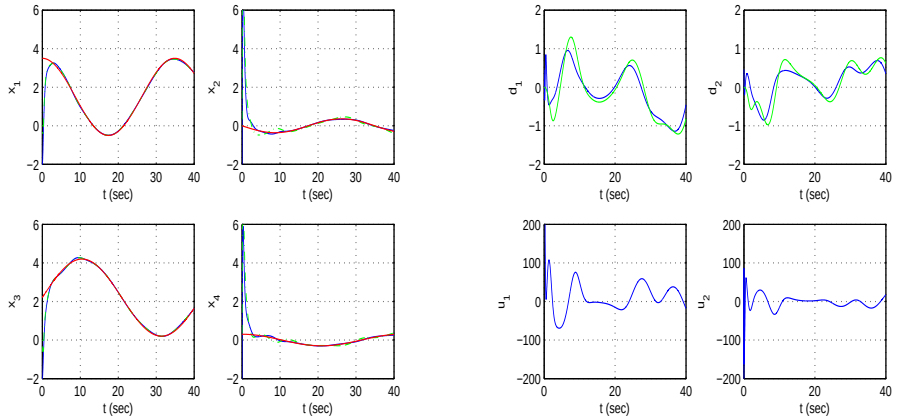

(a) **(b)**

Figure 5: Tracking of setpoint 4 by the 2-link robotic exoskeleton (a) Convergence of the state variables x_1 to x_4 (blue lines) to the reference setpoints (red lines) and KF-estimated state variables (green lines), (b) top diagrams: Kalman Filter-based estimation of disturbance torques $\tilde{d}_1$ and $\tilde{d}_2$ (green lines) and real values of these perturbations (blue lines), bottom diagrams: control inputs (torques) u_1 and u_2 applied to the joints of the exoskeleton

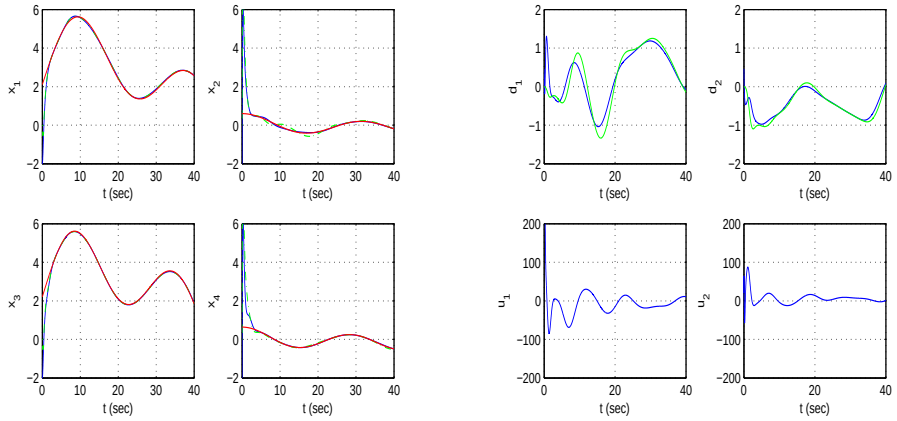

(a) **(b)**

Figure 6: Tracking of setpoint 5 by the 2-link robotic exoskeleton (a) Convergence of the state variables x_1 to x_4 (blue lines) to the reference setpoints (red lines) and KF-estimated state variables (green lines), (b) top diagrams: Kalman Filter-based estimation of disturbance torques $\tilde{d}_1$ and $\tilde{d}_2$ (green lines) and real values of these perturbations (blue lines), bottom diagrams: control inputs (torques) u_1 and u_2 applied to the joints of the exoskeleton

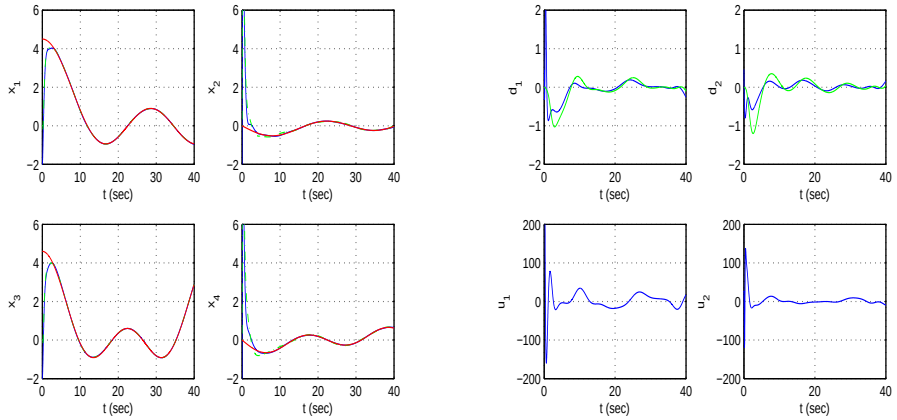

(a) **(b)**

Figure 7: Tracking of setpoint 6 by the 2-link robotic exoskeleton (a) Convergence of the state variables x_1 to x_4 (blue lines) to the reference setpoints (red lines) and KF-estimated state variables (green lines), (b) top diagrams: Kalman Filter-based estimation of disturbance torques $\tilde{d}_1$ and $\tilde{d}_2$ (green lines) and real values of these perturbations (blue lines), bottom diagrams: control inputs (torques) u_1 and u_2 applied to the joints of the exoskeleton

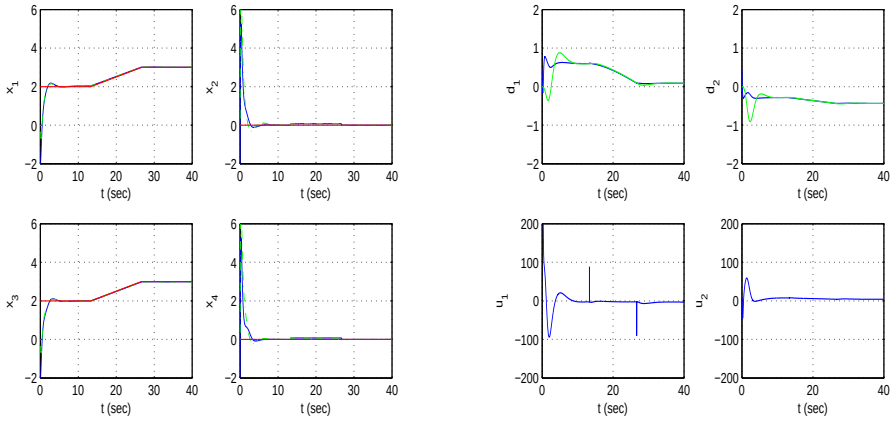

(a) **(b)**

Figure 8: Tracking of setpoint 7 by the 2-link robotic exoskeleton (a) Convergence of the state variables x_1 to x_4 (blue lines) to the reference setpoints (red lines) and KF-estimated state variables (green lines), (b) top diagrams: Kalman Filter-based estimation of disturbance torques $\tilde{d}_1$ and $\tilde{d}_2$ (green lines) and real values of these perturbations (blue lines), bottom diagrams: control inputs (torques) u_1 and u_2 applied to the joints of the exoskeleton

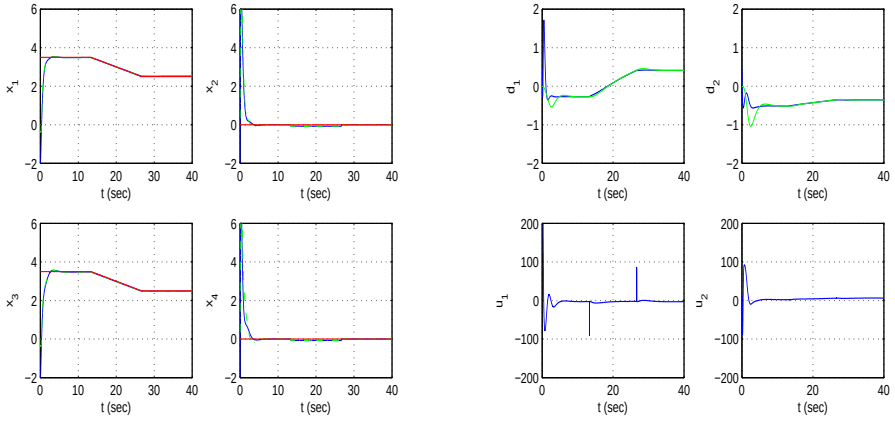

(a) **(b)**

Figure 9: Tracking of setpoint 8 by the 2-link robotic exoskeleton (a) Convergence of the state variables x_1 to x_4 (blue lines) to the reference setpoints (red lines) and KF-estimated state variables (green lines), (b) top diagrams: Kalman Filter-based estimation of disturbance torques $\tilde{d}_1$ and $\tilde{d}_2$ (green lines) and real values of these perturbations (blue lines), bottom diagrams: control inputs (torques) u_1 and u_2 applied to the joints of the exoskeleton

Table II				
Tracking RMSE for the robot under time-delay set $2{\cdot}\tau_d$				
	$RMSE_{x_1}$	$RMSE_{x_3}$	$RMSE_{\tilde{d}_1}$	$RMSE_{\tilde{d}_2}$
test_1	0.0041	0.0015	0.0346	0.0416
test_2	0.0015	0.0070	0.0230	0.0680
test_3	0.0096	0.0021	0.0923	0.0541
test_4	0.0038	0.0043	0.0692	0.0567
test_5	0.0028	0.0016	0.0231	0.0539
test_6	0.0049	0.0039	0.0324	0.0268
test_7	0.0015	0.0029	0.0002	0.0001
test_8	0.0018	0.0038	0.0001	0.0001

Table III				
Tracking RMSE for the robot under time-delay set $3{\cdot}\tau_d$				
	$RMSE_{x_1}$	$RMSE_{x_3}$	$RMSE_{\tilde{d}_1}$	$RMSE_{\tilde{d}_2}$
test_1	0.0043	0.0016	0.0366	0.033
test_2	0.0014	0.0072	0.0238	0.0707
test_3	0.0090	0.0022	0.0996	0.0588
test_4	0.0038	0.0044	0.0684	0.0568
test_5	0.0027	0.0015	0.0235	0.0530
test_6	0.0043	0.0040	0.0361	0.0294
test_7	0.0015	0.0029	0.0002	0.0001
test_8	0.0018	0.0038	0.0002	0.0001

Table IV				
Tracking RMSE for the robot under time-delay set $4{\cdot}\tau_d$				
	$RMSE_{x_1}$	$RMSE_{x_3}$	$RMSE_{\tilde{d}_1}$	$RMSE_{\tilde{d}_2}$
test_1	0.0043	0.0016	0.0366	0.0433
test_2	0.0014	0.0072	0.0238	0.0707
test_3	0.0094	0.0022	0.0896	0.0589
test_4	0.0038	0.0044	0.0684	0.0568
test_5	0.0027	0.0015	0.0235	0.0530
test_6	0.0043	0.0040	0.0361	0.0294
test_7	0.0015	0.0029	0.0002	0.0001
test_8	0.0018	0.0038	0.0002	0.0001

5 Conclusions

The article has developed a novel solution for the reliable functioning of robotic exoskeletons when time-delayed forces and torques affect this robotic mechanism. The proposed method has been based on the differential flatness properties of the exoskeleton's dynamic model and has allowed for designing a stabilizing feedback controller and a convergent disturbance observer for this robotic system. A two-link exoskeleton has been considered as a case study. By proving that this robotic system is differentially flat it has been confirmed that it can be transformed into the input-output linearized form or equivalently in the linear canonical (Brunovsly) form. In the latter description of the exoskeleton's dynamics, controllability and observability is also ensured. Thus, one can solve the control problem for the exoskeleton by applying the pole-placement (eigenvalues assignment method), and can treat optimally the associated states' and disturbances' estimation problems with the use of Kalman Filtering.

The use of the Kalman Filter's recursion in the flatness-based linearized state-space model of the robot, jointly with flatness-based inverse transformations which return the state estimates of the initial nonlinear

model of the exoskeleton is also known as Derivative-free nonlinear Kalman Filter. A significant problem in the exoskeleton's functioning was the compensation of unmodelled disturbance forces exerted on its free-end, as well the compensation of the associated disturbance torques which were transferred to its joints. Such disturbance forces and torques could be also be subject to unknown time-delays. By redesigning the aforementioned Kalman Filter as a disturbance observer it has become possible to estimate in real-time the variation of such perturbation forces and torques. Moreover, by including additional terms in the flatness-based controller of the robotic exoskeleton, being based on the disturbances' estimates, the compensation of the perturbations' effects has been achieved and the minimization of the setpoints' tracking error for the state variables of the exoskeleton has been enabled.

Statement: The authors of the article "Flatness-based disturbance observer for exoskeleton robots under time-delayed contact forces" declare that to their knowledge no conflict of interest exists with third parties about the content, results and methods of the above noted manuscript.

References

[1] G. Rigatos and K. Busawon, Robotic manipulators and vehicles: Control, estimation and filtering, Springer, 2018.

[2] G. Rigatos, Nonlinear control and filtering using differential flatness approaches: applications to electromechanical systems, Springer, 2015.

[3] W. Meng, Q. Liu, Z. Zhou, Q. Ai, B. Sheng, and S. Xie, Recent development of mechanisms and control strategies for robot-assisted lower limb rehabilitation, Mechatronics, Elsevier, vol. 31, pp. 132–145, 2015

[4] Y. Long and Y. Peng, Extended state observer-based nonlinear terminal sliding-mode control with feedforward with feedforward compensation for lower extremity exoskeleton, IEEE Access, vol. pp. 1-10, 2021

[5] G. Zhang, P. Yang, J. Wang and J. Sun, Multivariable finite-time control of 5-DOF upper limb exoskeleton based on linear extended state observer, IEEE Access, vol. 6, pp. 43213-43221 2018.

[6] C.F. Chen, Z.J. Du, L. He, J.O. Wang, D.M. Wu and W. Dong, Active disturbance rejection with fast terminal sliding-mode control for a lower-limb exoskeleton in swing-phase, IEEE Access, vol. 7, pp. 72343-72357, 2019.

[7] P. Yang,, X. Ma, J. Wang, G. Zhang, Y. Zhang and L. Chen, Disturbance observer-based terminal sliding-mode control of a 5-DOF upper-limb exoskeleton robot, IEEE Access, vol. 7, pp. 62813-62889, 2019.

[8] Z. Li, C.Y. Su, L. Wang, Z. Chen and T. Choi, Nonlinear disturbance observer-based control design for a robotic exoskeleton incorporating fuzzy approximator, IEEE Transactions on Industrial Electronics, vol. 62, o. 9, pp. 5763-5775, 2015.

[9] B. Brajimi, H. DrisellL.K El-Bojairimi, M. Saad and A. Brahimi, Novel adaptive impednance control for exoskeleton robot for rjabilization using a using a nonlinear time-delay observer, ISA Transactions, Elsevier, vol. 108, pp. 381-392, 2021.

[10] Y. Wang, H. Wang and Y. Tian, Nonlinear disturbance observer-based flexible boundary prescribed performance control for a lower limb exoskeleton, Intl. Journal of Systems Science, Taylor and Francis, pp. 1-15, 2021.

[11] N. Masoud, P. Mattson, C. Smith and M. Isaksson, On stability and performance of disturbance observer-based dynamic load torque compensation for assistive exoskeleton: A hybrid approach, Mechatronics, Elsevier, vol. 63, pp. 102373-102387, 2020.

[12] S. Hun, H. Wang and Y. Tian, A linear discrete-time extended state observer-based intelligent PD controller for a 12DOFs lower-limb exoskeleton LLF-RePA, Mechanican Systems and Signal Processing, Elsevier, vol. 138, pp. 106547-106561, 2020.

[13] F. Just, O. Ozen, F. Bosch, H. Bobrovsky,V. Klamroth-Morganska, R. Reiner and G. Rauter, Exoskeleton transparency: feed-forward compensation vs. disturbance observer, Automatisierungstechnik, De Gruyter, vol. 66, no. 12, pp. 1014-1026, 2018.

[14] F. Sudo, H.J. Yap, R.A.R. Ghazilla and N. Ahmad, Exoskeleton robot control for synchronous walking assistance in repetitive manual handling works based on dual Unscented Kalman Filter, Plos One, vol. 13, no. 7, pp. e0200193, 2019.

[15] S. Ahma, H. Wang and Y. Tian, Model-free control using time-delay estimation and fractional-order nonsingular fast terminal sliding-mode for uncertain ower-limb exoskeleton, Journal of Vibration and Control, Sage Publications, vol. 24 no 22, pp. 5273-5290, 2018

[16] M. Saadatzi, D.C. Long and O. Celik, Comparison of human-robot interaction torque estimation method in a wrist rehabilitation exoskeleton, Journal of Intelligent and Robotic Systems, Springer, vol. 94, pp. 565–581, 2018.

[17] J. Chan, Y Huang, X. Guo, S. Zhou and L. Jia, Parameter identification and adaptive compliant control of rehabilitation exoskeleton based on multiple sensors, Measurement, Elsevier, vol. 159, pp. 107765-107777, 2020.

[18] C. Liang and T. Hsiao, Admittance control of power exoskeletons based on joint torque estimation, IEEE Access vol.8, pp. 94404-94414, 2020.

[19] G.W. Zhang, P. Yang, J.Wang, J.F. Sun and Y. Zhang, Integrated observer-based fixed-time control with backstepping method for exoskeleton robot, Intl. Jounal of Automation and Computing, Springer, vol. 17, no. 1, pp. 71-82, 2020.

[20] Q. Wu, B. Chen and H. Wu, Neural network-enhanced toeque estimation control of a soft wearable exoskeleton for elbow assistance, Mechatronics, Elsevier, vol. 63, pp.102279-102288, 2018.

[21] B. Ugurlu, N. Nishimura, K. Hyodo, M. Kawanishi and T. Narikoyo, Proof of concept for robot-aided upper-limb rehabilization using disturbance observers, IEEE Transactions on Human-Machine Systems, vol. 45, no. 1,pp. 110-118, 2015

[22] J. Vantili, C. Giraldi, E. Aertbelien, F. de Groote, and J.J. de Schutter, Estimating contact forces and moments for walking robots and exoskeletons using complementary energy methods, IEEE Robotics and Automation Letters, vol. 3, no. 4, pp. 3410-3417, 2018.

[23] J. Wu, J. Huang, Y. Wang, and K. Xing, Nonlinear Disturbance Observer-Based Dynamic Surface Control for Trajectory Tracking of Pneumatic Muscle System, IEEE Transactions on Control Systems Technology, vol. 23, no. 2, pp. 440-455, 2014

[24] J. Rudolph, Flatness Based Control of Distributed Parameter Systems: Examples and Computer Exercises from Various Technological Domains, Shaker Verlag, Aachen, 2003.

[25] H. Sira-Ramirez and S. Agrawal, Differentially Flat Systems, Marcel Dekker, New York, 2004.

[26] J. Lévine, On necessary and sufficient conditions for differential flatness, Applicable Algebra in Engineering, Communications and Computing, Springer, vol. 22, no. 1, pp. 47-90, 2011.

[27] J. Villagra, B. d'Andrea-Novel, H. Mounier and M. Pengov, Flatness-based vehicle steering control strategy with SDRE feedback gains tuned via a sensitivity approach, IEEE Transactions on Control Systems Technology, vol. 15, pp. 554-565, 2007.

[28] S. Bououden, D. Boutat, G. Zheng, J.P. Barbot and F. Kratz, A triangular canonical form for a class of 0-flat nonlinear systems, International Journal of Control, Taylor and Francis, vol. 84, no. 2, pp. 261-269, 2011.

[29] G.G. Rigatos and S.G. Tzafestas, Extended Kalman Filtering for Fuzzy Modelling and Multi-Sensor Fusion, Mathematical and Computer Modelling of Dynamical Systems, Taylor & Francis, vol. 13, pp. 251-266, 2007.

[30] M. Basseville and I. Nikiforov, Detection of abrupt changes: Theory and Applications, *Prentice-Hall*, 1993.

[31] G. Rigatos and Q. Zhang, Fuzzy model validation using the local statistical approach, Fuzzy Sets and Systems, Elsevier, vol. 60, no.7, pp. 882-904, 2009.

[32] G.G. Rigatos, A derivative-free Kalman Filtering approach to state estimation-based control of nonlinear dynamical systems, IEEE Transactions on Industrial Electronics, vol. 59, no. 10, pp. 3987 - 3997, 2012.

[33] G Rigatos, M Abbaszadeh, J Pomares, P Wira, A nonlinear optimal control approach for a lower-limb robotic exoskeleton, World Scientific, vol. 17, no. 5, pp. 2050018, 2020.

[34] F. Nicolaum W. Respondek and J.P. Barbot, How to minimally modify a dynamical system when constructing flat inputs, Internattional Journal of Robust and Nonlinear Control, J. Wiley, 2022.

[35] C. Letller nd J.P. Barbot, Optimal flatness placement of sensors and actuators for controlling chaotic systemsm Chaos, AIP Publications, vol. 31, no. 10, article No 103114, 2021.

[36] F. Nicolau, W. Respondek and J.P. Barbot, Construction of flat inputs for mechanical systems, 7th IFAC Workshop on Lagrangian and Hamiltonian methods for nonlinear control, Berlin, Germany, OCt. 2021

[37] J.O. Limaverde Filho, E.C.R. Fortaleza and M.C.M. Campos, A derivative-free nonlinear Kalman Filtering approach using flat inputs, International Journal of Control, Taylor and Francis 2021.

[38] J.P. Barbot, M. Fliess and T. Floquet, An algebraic framework for the design of nonlinear observers with uknown inputs, IEEE CDC 2007, IEEE 46th Intl. Conference on Decision and Control, New Orleans, USA, Dec. 2007

Appendix: Differentially flat inputs for the m-DOF robot under model disturbances

The model of the multi-DOF robotic exoskeleton is also a differentially flat system, having as flat outputs the turn angles of its joints [1][. When written in the input-output linearized form and when disturbance terms are taken into account the state-space model becomes

1-st joint:	2-nd joint:		m-th joint:
$\dot{z}_1 = z_2$	$\dot{z}_{r_1+1} = z_{r_1+2}$		$\dot{z}_{n-r_m+1} = z_{n-r_m+2}$
$\dot{z}_2 = z_3$	$\dot{z}_{r_1+2} = z_{r_1+3}$		$\dot{z}_{n-r_m+2} = z_{n-r_m+3}$
$\cdots$	$\cdots$	$\cdots$	$\cdots$
$\cdots$	$\cdots$		$\cdots$
$\dot{z}_{r_1-1} = z_{r_1}$	$\dot{z}_{r_1+r_-1} = z_{r_1+r_2}$		$\dot{z}_{n-1} = z_n$
$\dot{z}_{r_1} = f_1(z) +$	$\dot{z}_{r_1+r_2} = f_2(z) +$		$\dot{z}_n = f_m(z) +$
$+\sum_{j=1}^{m} G_{1j}(z)u_j + \tilde{d}_1$	$+\sum_{j=1}^{m} G_{2j}(z)u_j + \tilde{d}_2$		$+\sum_{j=1}^{m} G_{mj}(z)u_j + \tilde{d}_m$

(56)

where $r_1 + r_2 + \cdots r_m = n$. The cumulative (virtual) control inputs of the previous state-space model are defined as: $v_1 = f_1(z) + \sum_{j=1}^{m} G_{1j}(z)u_j$, $v_2 = f_2(z) + \sum_{j=1}^{m} G_{2j}(z)u_j$, $\cdots$ $v_m = f_m(z) + \sum_{j=1}^{m} G_{mj}(z)u_j$, while there exist also the additive disturbance inputs $\tilde{d}_1$, $\tilde{d}_2$ and $\tilde{d}_3$.

The state-space model of the m-DOF robotic exoskeleton is extended by considering as additional state variables for the i-th joint the associated disturbance term and its time-derivatives up to order q_i. This concept maintains the model's consistency because each disturbance variable can be indeed substituted by the associated q_i-th order time-derivative and the related initial conditions.

The new state variables of the robotic model are: for the first joint $z_{n+1} = \tilde{d}_1$, $z_{n+2} = \dot{\tilde{d}}_1$, $\cdots$, $z_{n+q_1} = \tilde{d}^{(q_i-1)}$ with $\tilde{d}^{(q_i)} = f_{d_1}$. For the second joint: $z_{n+q_1+1} = \tilde{d}_2$, $z_{n+q_1+2} = \dot{\tilde{d}}_2$, $\cdots$, $z_{n+q_1+q_2} = \tilde{d}_2^{(q_2-1)}$ with $\tilde{d}^{(q_2)} = f_{d_2}$ and continuing in a similar manner for the m-th joint one has $z_{n+q_1+q_2+\cdots+q_{n-1}+1} = \tilde{d}_m$, $z_{n+q_1+q_2+\cdots+q_{m-1}+2} = \dot{\tilde{d}}_m$, $\cdots$, $z_{n+q_1+q_2+\cdots+q_m} = \tilde{d}^{(q_m-1)}$ with $\tilde{d}_m^{(q_m)} = f_{d_m}$.

This allows to rewrite the system into a new state-space form in which the disturbances become new control inputs. Next the following notations are used for the state variables and the control inputs of the m-DOF robot: $Z_1 = [z_1, z_2, \cdots, z_{r_i}]^T$, $Z_2 = [z_{r_1+1}, z_{r_1+2}, \cdots, z_{r_1+r_2}]^T$, $\cdots$ $Z_m = [z_{r_m-1}, z_{r_m}, \cdots, z_n]^T$ and $U = [v_1, v_2, \cdots, v_m]^T$.

Besides the following notations are used for the disturbance variables and the disturbance inputs of the m-DOF robot: $\tilde{Z}_1 = [\tilde{d}_1, \dot{\tilde{d}}_1, \cdots, \tilde{d}_1^{(q_1-1)})]^T$, $\tilde{Z}_2 = [\tilde{d}_2, \dot{\tilde{d}}_2, \cdots, \tilde{d}_2^{(q_2-1)})]^T$, $\cdots$ $\tilde{Z}_m = [\tilde{d}_m, \dot{\tilde{d}}_m, \cdots, \tilde{d}_m^{(q_m-1)})]^T$ and $\tilde{U} = [f_{d_1}, f_{d_2}, \cdots, f_{d_m}]^T$.

Then, the following extended state-space model of the robotic system is obtained:

$$\begin{pmatrix} \dot{Z}_1 \\ \dot{Z}_2 \\ \cdots \\ \dot{Z}_n \\ \dot{\tilde{Z}}_1 \\ \dot{\tilde{Z}}_2 \\ \cdots \\ \dot{\tilde{Z}}_n \end{pmatrix} = \begin{pmatrix} A_{11} & 0_{r_1\times r_2} & \cdots & 0_{r_1\times r_m} & A_{21} & 0_{r_1\times q_2} & \cdots & 0_{r_1\times q_m} \\ 0_{r_2\times r_1} & A_{12} & \cdots & 0_{r_2\times r_m} & 0_{r_2\times q_1} & A_{22} & \cdots & 0_{r_2\times q_m} \\ \cdots & \cdots & \cdots & \cdots & \cdots & \cdots & \cdots & \cdots \\ 0_{r_m\times r_1} & 0_{r_m\times r_2} & \cdots & A_{1m} & 0_{r_m\times q_1} & 0_{r_m\times q_2} & \cdots & A_{2m} \\ 0_{q_1\times r_1} & 0_{q_1\times r_2} & \cdots & 0_{q_1\times r_m} & \tilde{A}_{21} & 0_{q_1\times q_2} & \cdots & 0_{q_1\times q_m} \\ 0_{q_2\times r_1} & 0_{q_2\times r_2} & \cdots & 0_{q_2\times r_m} & 0_{q_2\times q_1} & \tilde{A}_{22} & \cdots & 0_{q_2\times q_m} \\ \cdots & \cdots & \cdots & \cdots & \cdots & \cdots & \cdots & \cdots \\ 0_{q_m\times r_1} & 0_{q_m\times r_2} & \cdots & 0_{q_m\times r_m} & 0_{q_m\times q_1} & 0_{q_m\times q_2} & \cdots & \tilde{A}_{2m} \end{pmatrix} \begin{pmatrix} Z_1 \\ Z_2 \\ \cdots \\ Z_m \\ \tilde{Z}_1 \\ \tilde{Z}_2 \\ \cdots \\ \tilde{Z}_m \end{pmatrix} + \\ + \begin{pmatrix} B_{11} \\ B_{12} \\ \cdots \\ B_{1m} \\ 0_{q_1\times m} \\ 0_{q_2\times m} \\ \cdots \\ 0_{q_m\times m} \end{pmatrix} U + \begin{pmatrix} 0_{r_1\times m} \\ 0_{r_2\times m} \\ \cdots \\ 0_{r_m\times m} \\ \tilde{B}_{11} \\ \tilde{B}_{12} \\ \cdots \\ \tilde{B}_{1m} \end{pmatrix} \tilde{U} \tag{57}$$

or in concise form $\dot{Z} = f(Z) + \gamma_1(Z)U + \gamma_2(Z)\tilde{U}$.

where all matrices denoted as $0_{r_i\times r_j}$, $0_{r_i\times q_j}$, $0_{q_i\times q_j}$ or $0_{q_i\times r_j}$ have all their elements equal to zero, while the following matrices are also defined:

$$A_{11}=\begin{pmatrix}0_{(r_1-1)\times 1} & I_{(r_1-1)\times(r_1-1)}\\ 0 & 0_{1\times(r_1-1)}\end{pmatrix}\quad A_{21}=\begin{pmatrix}0_{(r_1-1)\times 1} & I_{(r_1-1)\times(r_1-1)}\\ 1 & 0_{1\times(r_1-1)}\end{pmatrix} \tag{58}$$

$$A_{12}=\begin{pmatrix}0_{(r_2-1)\times 1} & I_{(r_2-1)\times(r_2-1)}\\ 0 & 0_{1\times(r_2-1)}\end{pmatrix}\quad A_{22}=\begin{pmatrix}0_{(r_2-1)\times 1} & I_{(r_2-1)\times(r_2-1)}\\ 1 & 0_{1\times(r_2-1)}\end{pmatrix} \tag{59}$$

$$\cdots\quad\cdots\quad\cdots\quad\cdots\quad\cdots$$

$$A_{1m}=\begin{pmatrix}0_{(r_m-1)\times 1} & I_{(r_m-1)\times(r_m-1)}\\ 0 & 0_{1\times(r_m-1)}\end{pmatrix}\quad A_{22}=\begin{pmatrix}0_{(r_m-1)\times 1} & I_{(r_m-1)\times(r_m-1)}\\ 1 & 0_{1\times(r_m-1)}\end{pmatrix} \tag{60}$$

Besides, matrices $B_{1j}\in R^{r_j\times m}$ have all their elements equal to 0, apart from elements $b_{r_j\times j}$ which is equal to 1. Equivalently one has

$$\begin{gathered}\tilde{A}_{21}=\begin{pmatrix}0_{(q_1-1)\times 1} & I_{(q_1-1)\times(q_1-1)}\\ 1 & 0_{1\times(q_1-1)}\end{pmatrix}\qquad \tilde{A}_{22}=\begin{pmatrix}0_{(q_2-1)\times 1} & I_{(q_2-1)\times(q_2-1)}\\ 1 & 0_{1\times(q_2-1)}\end{pmatrix}\\ \cdots\quad\cdots\qquad\qquad \tilde{A}_{2m}=\begin{pmatrix}0_{(q_m-1)\times 1} & I_{(q_m-1)\times(q_m-1)}\\ 1 & 0_{1\times(q_m-1)}\end{pmatrix}\end{gathered} \tag{61}$$

Matrices $\tilde{B}_{ij}\in R^{q_j\times m}$, $j=1.2.\cdots,m$ have all their elements equal to 0, apart from element $\tilde{b}_{q_j\times j}$ which is equal to 1.

By denoting as $Z=[Z_1,Z_2,\cdots,Z_m,\tilde{Z}_1,\tilde{Z}_2,\cdots,\tilde{Z}_m]$ as the extended state vector of the system, the measurement equation of the extended state-space model of the m-DOF robotic exoskeleton becomes

$$Z^m=C_{m\times(n+q_1+q_2+\cdots+q_m)}\cdot Z \tag{62}$$

where matrix C has all its elements equal to 0 apart from elements $C_{1,1}, C_{2,r_1+1}, C_{3,r_1+r_2+1},\cdots,C_{m,n-r_m+1}$, which are equal to 1. This demonstrates that the measured variables are again the turn angles of the robot, as in the case of the disturbance-free robotic model. It can be confirmed that after introducing the additional control inputs $\tilde{U}$, the vector that comprises the joint angles and the additive input perturbations $Y=[z_1,z_{r_1+1},z_{r_1+r_2+1},\cdots,z_{n-r_m+1},\tilde{d}_1,\tilde{d}_2,\tilde{d}_3,\cdots,\tilde{d}_m]$ is a flat outputs vector of the extended system.

Indeed from the definition of the state-vector of the extended system $Z=[Z_1,Z_2,\cdots,Z_m,\tilde{Z}_1,\tilde{Z}_2,\tilde{Z}_m]$ it is apparent that all state vector elements are differential functions of the above-noted flat outputs vector Y. Besides, it holds that

$$\begin{gathered}z_1^{(r_1)}=v_1+\tilde{d}_1\Rightarrow v_1=z_1^{(r_1)}-\tilde{d}_1\\ z_{r_1+1}^{(r_2)}=v_2+\tilde{d}_2\Rightarrow v_2=z_{r_1+1}^{(r_2)}-\tilde{d}_2\\ \cdots\ \cdots\ \cdots\\ z_{n-r_m+1}^{(r_m)}=v_m+\tilde{d}_m\Rightarrow v_m=z_{n-r_m+1}^{(r_m)}-\tilde{d}_m\end{gathered} \tag{63}$$

Consequently, the control inputs of the extended state-space model of the system are differential functions of the flat outputs and thus the extended state-space model is a differentially flat system.

Finally, it will be proven that under the disturbances effects the robotic exoskeleton is a system with differentially flat inputs. For an observable noninear system in the form

$$\begin{gathered}\dot{z}=f(x,u)\\ y_i=h_i(x)\end{gathered} \tag{64}$$

where $i = 1, 2, \cdots, m$ and $x \in R^n$, $u \in R^m$, $y_i \in R$ with f to be a smooth vector field, and h_i to be also smooth functions, differentially flat inputs can be defined if there exist m input vector fields $\gamma_i(x)$ and the resulting input-affine nonlinear MIMO system

$$\dot{x} = f(x, 0) + \sum_{i=1}^{m} \gamma_i(x) u_{j_f} \tag{65}$$

is differentially flat, with y_i to be flat outputs. In such a case the inputs u_{j_f} are the *flat inputs* of the system [34-36].

The extended state-space model of the robotic exoskeleton is differentially flat and observable and can be used for developing an unknown inputs observer (disturbance observer) [37-38] . Moreover, using its state-space description of Eq. (57) and by comparing it to the anticipated form for systems with differentially flat inputs which has been given in Eq. (65), the control inputs $U = [f_{d_1}, \tilde{f_{d_2}}, \cdots, f_{d_n}]^T$ can be considered to be differentially flat inputs for the multi-DOF robotic system under the effect of model disturbances.